BOUNDARY SLIPPAGE FOR IMPROVING THE LOAD AND FRICTION PERFORMANCE OF A STEP BEARING

Yongbin Zhang
College of Mechanical and Energy Engineering, Changzhou University (Formerly Jiangsu Polytechnic University), 213016, Changzhou, Jiangsu Province, China
E-mail: engmech1@sina.com

Received February 2010, Accepted September 2010
No. 10-CSME-07, E.I.C. Accession 3170

ABSTRACT

The present paper proposes a new type of step bearing by specifically modifying the interfacial condition between the fluid film and the bearing surface and introducing the boundary slippage at those interfaces. Analysis for the load-carrying capacity and friction coefficient is presented for this kind of bearing. The comparison of the obtained analytical results with the conventional (no-slippage) step bearing results shows that modifying the interfacial condition and introducing the boundary slippage at the specific bearing surfaces can significantly increase the load-carrying capacity and reduce the friction coefficient of a step bearing. Design guideline, the load-carrying capacity and the friction coefficient are also presented for this bearing at optimum condition which reaches the maximum load-carrying capacity.

Keywords: boundary slippage; hydrodynamic step bearing; load-carrying capacity; friction coefficient.

LIMITATION DU GLISSEMENT POUR L'AMÉLIORATION DE LA PERFORMANCE DE LA CAPACITÉ DE CHARGE ET DE LA FRICTION D'UNE CRAPAUDINE

RÉSUMÉ

On propose un nouveau type de crapaudine par la modification spécifique de la condition des interfaces entre le film lubrifiant et la surface du palier, et l'introduction de la limitation du glissement à ces interfaces. On effectue une analyse de la capacité de charge et le coefficient de friction pour ce type de paliers. La comparaison des résultats obtenus avec ceux des paliers conventionnels (non glissant) démontrent que la modification de l'interface et l'introduction de la limitation de glissement à des surfaces spécifiques du palier peut augmenter de façon significative la capacité de charge et réduire le coefficient de friction du palier. En plus des principes de design, la capacité de charge et le coefficient de friction est aussi présentée pour une condition optimale du palier, lequel atteint la capacité maximale de charge.

Mots-clés : limitation de glissement, hydrodynamique, crapaudine, capacité de charge, coefficient de friction.

Nomenclature

c_1, c_2	integral constants
f	friction coefficient
G	function of ψ, Eq. (20)
G_1	maximum value of G
h_a	film thickness in the fluid inlet zone
h_b	film thickness in the fluid outlet zone
K_u	$3(U-\lambda_\tau/2)$
l_1	width of the fluid outlet zone i.e. the "A" sub-zone
l_2	width of the fluid inlet zone i.e. the "B" sub-zone
$\bar{lu}$	average velocity of the fluid films at the upper and lower bearing surfaces
p	fluid film pressure
P	dimensionless fluid film pressure
$p_{\max}$	maximum fluid film pressure
$P_{\max}$	dimensionless maximum fluid film pressure
q	fluid mass flow through the contact per unit contact length
q_v	fluid volume flow through the contact per unit contact length
r_h	h_a/h_b
u	sliding speed between two bearing surfaces
U	dimensionless sliding speed between two bearing surfaces
w	carried load per unit contact length of the bearing
W	dimensionless carried load per unit contact length of the bearing
x	coordinate shown in Fig. 1
α	$h_a/(l_1+l_2)$
ρ	fluid density
λ_1	$3\tau_{sa}/(2h_a)-3u\eta/h_a^2-3\eta q_v/h_a^3$
λ_2	$-3\tau_{sb}/(2h_b)-3\eta q_v/h_b^3$
λ_τ	τ_{sa}/τ_{sb}
ψ	l_1/l_2
ψ_{opt}	optimum value of ψ at which the load-carrying capacity reaches the maximum
ϕ_τ	$\tau_{sa,A}/\tau_{sb}$
η	fluid viscosity
τ	shear stress
τ_{sa}	contact-fluid interfacial shear strength at the stationary bearing surface in the fluid inlet zone
$\tau_{sa,A}$	contact-fluid interfacial shear strength at the stationary bearing surface in the fluid outlet zone
τ_{sb}	contact-fluid interfacial shear strength at the moving bearing surface
Δu_a	fluid film slipping velocity at the stationary bearing surface i.e. the upper bearing surface
Δu_b	fluid film slipping velocity at the moving bearing surface i.e. the lower bearing surface

Subscripts

a	at the upper bearing surface
b	at the lower bearing surface
A	in the "A" sub-zone
B	in the "B" sub-zone
conv	for conventional no-slippage hydrodynamic step bearing
slip	for present slippage hydrodynamic step bearing

1. INTRODUCTION

Boundary slippage has been paid attention in a hydrodynamic contact in recent years. For example, Zhang and Wen analyzed the boundary slippage phenomena and effect in a hydrodynamic line contact and found that the occurrence of the boundary slippage at the contact-fluid interface can greatly reduce the load-carrying capacity of a hydrodynamic line contact especially at large slide-roll ratios[1–3]; Also they found that the interfacial slippage can greatly reduce the friction coefficient of a hydrodynamic line contact especially at heavy loads and large slide-roll ratios [1, 4]. Experiments proved the occurrence of boundary slippage in hydrodynamic concentrated contacts [5–7]. Those experiments confirmed the analytical finding of Zhang and Wen [1] and found that the boundary slippage reduced the load-carrying capacity of a hydrodynamic contact. It shows that boundary slippage is not beneficial to the load-carrying capacity of a hydrodynamic contact.

In a hydrodynamic contact, boundary slippage is the result of the shear stress at the fluid-contact interface exceeding the contact-fluid interfacial shear strength [1]. It practically occurs in a hydrodynamic contact since the contact-fluid interfacial shear strength is actually rather limited [8]. Zhang proposed that boundary slippage should be considered in the theoretical and experimental studies of hydrodynamic lubricated contacts[9]; It might need the conventional hydrodynamic lubrication theory to be revised [9].

In a recent paper, Zhang proposed the possibility of using the boundary slippage to generate the hydrodynamic load-carrying capacity [10]. He suggested that hydrodynamic film can even be formed between two parallel plane surfaces sliding against one another to carry the contact load simply depending on the boundary slippage at the contact-fluid interface. He suggested that in this load-carrying capacity generation mechanism boundary slippage should be designed at the stationary contact surface in the hydrodynamic contact inlet zone; Thus the contact-fluid interfacial shear strength at the inlet zone stationary contact surface needs to be significantly low. Otherwise, the load-carrying capacity is unable to be generated in such a contact. This finding obviously challenges the concept of conventional hydrodynamic theory that the load-carrying capacity is unable to be generated between two parallel plane surfaces sliding against one another.

The present paper proposes another type of design method to further improve the load-carrying capacity of a hydrodynamic contact by using the boundary slippage. In this method, boundary slippage is not only designed at the stationary contact surface in the hydrodynamic inlet zone, but also designed at the moving contact surface in the hydrodynamic outlet zone. Application example of this design is for a hydrodynamic step bearing. The present paper proposes a new type of hydrodynamic step bearing by using this boundary slippage design which shows the improved load-carrying capacity and reduced friction coefficient compared to conventional (no-slippage) hydrodynamic step bearing in the same operating condition. An analysis is presented for the load-carrying capacity and friction coefficient of this type of step bearing. Corresponding results are obtained for several groups of operational parameter values. These results are compared to conventional hydrodynamic step bearing results for the same operating condition.

2. CONFIGURATION OF THE NEW TYPE OF HYDRODYNAMIC STEP BEARING

Figure 1 demonstrates the profile of the present proposed new type of hydrodynamic step bearing. The difference of this bearing from conventional hydrodynamic step bearing is that at the stationary bearing surface in the fluid inlet zone the contact-fluid interfacial shear strength is low so that boundary slippage occurs at that bearing surface, also at the moving bearing surface

in the fluid outlet zone the contact-fluid interfacial shear strength is low so that boundary slippage occurs at that bearing surface. At the other contact surfaces of this bearing, the contact-fluid interfacial shear strength is high enough so that boundary slippage is absent at those bearing surfaces. In Fig. 1, the upper bearing surface is stationary and the lower bearing surface is moving with the speed u, the fluid is entrained from the bearing inlet zone (i.e. the "B" sub-zone) into the bearing outlet zone (i.e. the "A" sub-zone), h_a is the fluid film thickness in the bearing inlet zone, h_b is the fluid film thickness in the bearing outlet zone, l_1 is the width of the bearing outlet zone, l_2 is the width of the bearing inlet zone, ($(l_1+l_2)$is the width of the whole bearing), τ_{sa} is the contact-fluid interfacial shear strength at the stationary bearing surface in the inlet zone, τ_{sb} is the contact-fluid interfacial shear strength at the lower bearing surface, and $\tau_{sa,A}$ is the contact-fluid interfacial shear strength at the stationary bearing surface in the outlet zone. The used coordinates are shown in Fig. 1.

3. ANALYSIS

An analysis is derived for the load-carrying capacity and the friction coefficient of the present proposed bearing. For comparison, the analysis is also presented for the load-carrying capacity and the friction coefficient of the conventional (no-slippage) hydrodynamic step bearing in the same operating condition. These analysis are based on the following assumptions:

(a) The flow is one-dimensional;
(b) The pressure across the film thickness is constant;
(c) The film inertia is negligible;
(d) The operating condition is steady-state and isothermal;
(e) The fluid is Newtonian.

3.1. Present Bearing

According to hydrodynamic mechanics [11] and the present bearing design, the shear stress at the upper bearing surface in the fluid inlet zone is:

$$\tau_{a,B}=\eta\frac{u}{h_a}+\frac{1}{2}\frac{dp}{dx}h_a=\tau_{sa} \tag{1}$$

where η is fluid viscosity and p is fluid pressure. The shear stress at the lower bearing surface in the fluid inlet zone is:

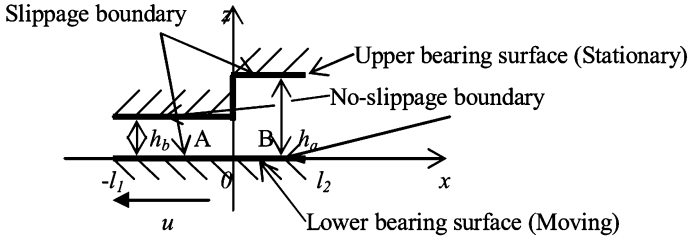

A-Fluid outlet zone, B-Fluid inlet zone

u-Moving speed

Fig. 1. Present proposed hydrodynamic step bearing with boundary slippage.

$$\tau_{b,B} = \eta \frac{u}{h_a} - \frac{1}{2}\frac{dp}{dx} h_a \tag{2}$$

The shear stress at the upper bearing surface in the fluid outlet zone is:

$$\tau_{a,A} = \eta \frac{u}{h_b} + \frac{1}{2}\frac{dp}{dx} h_b \tag{3}$$

The shear stress at the lower bearing surface in the fluid outlet zone is:

$$\tau_{b,A} = \eta \frac{u}{h_b} - \frac{1}{2}\frac{dp}{dx} h_b = \tau_{sb} \tag{4}$$

3.1.1. "B" Sub-zone

In the "B" sub-zone, the shear stresses at the upper and lower bearing surfaces can be respectively re-expressed as $\tau_{a,B} = \tau_{sa}$ and $\tau_{b,B} = \tau_{sa} - (dp/dx)h_a$. The boundary slipping velocities at the upper and lower bearing surfaces are respectively [1]:

$$\Delta u_{a,B} = \frac{\tau_{sa} h_a}{\eta} - \frac{h_a^2}{2\eta}\frac{dp}{dx} - u, \;\; \Delta u_{b,B} = 0 \tag{5}$$

According to the present bearing design, it should be satisfied that [1]:

$$\Delta u_{a,B} < 0, \;\; |\tau_{b,B}| < \tau_{sb} \tag{6}$$

It is assumed that the fluid film pressure influences on the fluid viscosity and density are negligible. Then the Reynolds equation in the "B" sub-zone is [1]:

$$\frac{\rho h_a^3}{\eta}\frac{dp}{dx} = 12\,\bar{lu}\;\; \rho h_a - 12q \tag{7}$$

where ρ is fluid density, q is the fluid flow rate through the contact and

$$\bar{lu} \;\; = \frac{\tau_{sa} h_a}{2\eta} - \frac{h_a^2}{4\eta}\frac{dp}{dx} - u \tag{8}$$

Substituting Eq. (8) into Eq. (7) and rearranging gives:

$$\frac{dp}{dx} = \lambda_1 \tag{9}$$

where $\lambda_1 = 3\tau_{sa}/(2h_a) - 3u\eta/h_a^2 - 3\eta q_v/h_a^3$ and q_v is the fluid volume flow rate through the contact per unit contact length.

Integrating Eq. (9) gives:

$$p = \lambda_1 x + c_1 \tag{10}$$

where c_1 is integral constant. From the boundary condition $p(l_2) = 0$ it is solved that $c_1 = -\lambda_1 l_2$. Then the fluid film pressure in the "B" sub-zone is:

$$p = \lambda_1 (x - l_2) \tag{11}$$

At $x = 0$, the fluid film pressure is $p(0) = -\lambda_1 l_2$.

3.1.2. For The "A" Sub-zone

In the "A" sub-zone, the Reynolds equation is [1]:

$$\frac{\rho h_b^3}{\eta} \frac{dp}{dx} = 12\, \bar{lu}\ \rho h_b - 12q \tag{12}$$

where

$$\bar{lu}\ = -\frac{\tau_{sb} h_b}{2\eta} - \frac{h_b^2}{4\eta} \frac{dp}{dx} \tag{13}$$

Substituting Eq. (13) into Eq. (12) and rearranging gives:

$$\frac{dp}{dx} = \lambda_2 \tag{14}$$

where $\lambda_2 = -3\tau_{sb}/(2h_b) - 3\eta q_v / h_b^3$.

Integrating Eq. (14) gives:

$$p = \lambda_2 x + c_2 \tag{15}$$

where c_2 is integral constant. From the boundary condition $p(-l_1) = 0$ it is solved that $c_2 = \lambda_2 l_1$. Then the fluid film pressure in the "A" sub-zone is:

$$p = \lambda_2 (x + l_1) \tag{16}$$

At $x = 0$, the fluid film pressure is $p(0) = \lambda_2 l_1$.

3.1.3. Fluid Volume Flow Rate through the Contact, Maximum Fluid Film Pressure and Carried Load per Unit Contact Length of the Bearing

According to the above derivation, it is equated that:

$$-\lambda_1 l_2 = \lambda_2 l_1 \tag{17}$$

Define $\psi = l_1 / l_2$ and $r_h = h_a / h_b$, it is solved from Eq. (17) that:

$$q_v = \frac{\tau_{sa} h_a^2 - 2u\eta h_a - \tau_{sb} h_a^2 r_h \psi}{2\eta \left(1 + r_h^3 \psi\right)} \tag{18}$$

The maximum fluid film pressure is calculated as:

$$p_{\max,slip} = p(0) = G(\psi) \frac{\tau_{sb} (l_1 + l_2)}{h_a} \tag{19}$$

where

$$G(\psi)=\frac{K_u\psi r_h^3-\frac{3}{2}r_h\psi}{(1+\psi r_h^3)(1+\psi)} \tag{20}$$

where $K_u=3(U-\lambda_\tau/2)$. Here, $U=u\eta/(\tau_{sb}h_a)$ and $\lambda_\tau=\tau_{sa}/\tau_{sb}$. The parameters U, K_u and G are dimensionless.

The carried load per unit contact length of the bearing is:

$$w_{slip}=\frac{p_{\max,slip}(l_1+l_2)}{2}=\frac{G(\psi)\tau_{sb}(l_1+l_2)^2}{2h_a} \tag{21}$$

3.1.4. Conditions for The Present Bearing

The fluid flow rate through the contact in Fig. 1 is negative i.e. $q_v<0$ since the fluid flow is opposite to the x coordinate direction. According to this and Eq. (18), we have:

$$\tau_{sa}<\frac{2u\eta}{h_a}+\tau_{sb}\psi r_h \tag{22}$$

From the condition $p(0)=-\lambda_1 l_2>0$, we have $\lambda_1<0$. Substituting the value of λ_1 derived in section 3.1.1 into this condition gives:

$$\tau_{sa}<\frac{2u\eta}{h_a}-\frac{\tau_{sb}}{r_h^2} \tag{23}$$

Comparison of Eq. (23) with Eq. (22) shows that Eq. (23) is the necessary condition for the hydrodynamic lubrication in the present bearing.

The shear stress at the lower bearing surface in the "B" sub-zone is calculated as:

$$\tau_{b,B}=\tau_{sa}-\frac{dp}{dx}h_a=\tau_{sa}+G(\psi)(1+\psi)\tau_{sb} \tag{24}$$

The condition for the absence of the boundary slippage at the lower bearing surface in the "B" sub-zone is:

$$\tau_{sb}>\tau_{sa}+G(\psi)(1+\psi)\tau_{sb} \tag{25}$$

The shear stress at the upper bearing surface in the "A" sub-zone is calculated as:

$$\tau_{a,A}=\tau_{sb}+\frac{dp}{dx}h_b=\tau_{sb}\left[1+\frac{G(\psi)}{r_h}\left(1+\frac{1}{\psi}\right)\right] \tag{26}$$

The condition for the absence of the boundary slippage at the upper bearing surface in the "A" sub-zone is:

$$\tau_{sa,A}>\tau_{sb}\left[1+\frac{G(\psi)}{r_h}\left(1+\frac{1}{\psi}\right)\right] \tag{27}$$

Equations (23), (25) and (27) are the conditions for the present bearing.

3.1.5. Friction Coefficient

The friction coefficient at the upper bearing surface is:

$$f_{a,slip} = \frac{\tau_{sa} l_2 + \tau_{sb} l_1 \left[1 + \frac{G(\psi)}{r_h}\left(1 + \frac{1}{\psi}\right)\right]}{w_{slip}} = \frac{2\alpha\left\{\lambda_\tau + \psi\left[1 + \frac{G(\psi)}{r_h}\left(1 + \frac{1}{\psi}\right)\right]\right\}}{G(\psi)(1+\psi)} \tag{28}$$

where $\alpha = h_a/(l_1 + l_2)$.

The friction coefficient at the lower bearing surface is:

$$f_{b,slip} = \frac{\tau_{sb} l_1 + \tau_{sb} l_2 [\lambda_\tau + G(\psi)(1+\psi)]}{w_{slip}} = 2\alpha\left[\frac{\lambda_\tau + \psi}{G(\psi)(1+\psi)} + 1\right] \tag{29}$$

3.1.6. Normalization

The parameters in the present study are normalized. Besides the above mentioned normalized parameters, the normalized parameters are listed as follows:

$$P = \frac{p h_a}{\tau_{sb}(l_1 + l_2)},\ W_{slip} = \frac{w_{slip} h_a}{\tau_{sb}(l_1 + l_2)^2},\ \phi_\tau = \frac{\tau_{sa,A}}{\tau_{sb}}$$

The dimensionless load per unit contact length carried by the bearing is:

$$W_{slip} = \frac{1}{2} G(\psi) \tag{30}$$

The dimensionless maximum fluid film pressure is:

$$P_{\max,slip} = G(\psi) = 2 W_{slip} \tag{31}$$

The conditions for the present bearing given in section 3.1.4 i.e. Eqs. (23), (25) and (27) are respectively normalized as follows:

$$\lambda_\tau < 2U - \frac{1}{r_h^2} \tag{32}$$

$$\lambda_\tau + G(\psi)(1+\psi) < 1 \tag{33}$$

$$\phi_\tau > 1 + \frac{G(\psi)}{r_h}\left(1 + \frac{1}{\psi}\right) \tag{34}$$

3.1.7. Maximum Load-Carrying Capacity

It is derived from Eq. (20) that the value of G reaches the maximum G_1 when ψ is taken as the following optimum value:

$$\psi_{opt} = \frac{K_u r_h^3 - G_1\left(r_h^3 + 1\right) - \frac{3}{2} r_h}{2 G_1 r_h^3} \tag{35}$$

where

$$G_1 = \frac{K_u r_h^3 - \frac{3}{2} r_h}{\left(r_h^{\frac{3}{2}} + 1\right)^2} \tag{36}$$

According to Eq. (30), the dimensionless load W_{slip} reaches the maximum $G_1/2$ when ψ is taken as the optimum value ψ_{opt}.

3.2. For Conventional (No-Slippage) Hydrodynamic Step Bearing

Conventional no-slippage hydrodynamic step bearing was studied quite early and analytical results for this bearing can be found from a lot of published books. This section only gives the final results for this bearing. Based on the above stipulated assumptions, the maximum fluid film pressure in this bearing is [11]:

$$p_{\max,conv} = p(0) = \frac{6u\eta l_1 (r_h - 1)}{h_b^2\left(\psi r_h^3 + 1\right)} \tag{37}$$

The load per unit contact length carried by this bearing is [11]:

$$w_{conv} = \frac{p_{\max,conv}(l_1 + l_2)}{2} = \frac{3u\eta l_1 (l_1 + l_2)(r_h - 1)}{h_b^2\left(\psi r_h^3 + 1\right)} \tag{38}$$

3.2.1. Normalization

Using the same normalization method as in section 3.1.6, the dimensionless load per unit contact length carried by this bearing is:

$$W_{conv} = \frac{w_{conv} h_a}{\tau_{sb}(l_1 + l_2)^2} = \frac{3U\psi r_h^2 (r_h - 1)}{(\psi + 1)\left(\psi r_h^3 + 1\right)} \tag{39}$$

The dimensionless maximum fluid film pressure in the bearing is:

$$P_{\max,conv}=\frac{p_{\max,conv}h_a}{\tau_{sb}(l_1+l_2)}=2W_{conv} \tag{40}$$

3.2.2. Friction Coefficient

The friction coefficient at the upper contact surface of this bearing is:

$$f_{a,conv}=\frac{\alpha\left\{U-W_{conv}(1+\psi)+\psi\left[Ur_h+\frac{W_{conv}}{r_h}\left(1+\frac{1}{\psi}\right)\right]\right\}}{W_{conv}(1+\psi)} \tag{41}$$

The friction coefficient at the lower contact surface of this bearing is:

$$f_{b,conv}=\frac{\alpha\left\{U+W_{conv}(1+\psi)+\psi\left[Ur_h-\frac{W_{conv}}{r_h}\left(1+\frac{1}{\psi}\right)\right]\right\}}{W_{conv}(1+\psi)} \tag{42}$$

4. RESULTS

4.1. Pressure Distribution In The Present Bearing

Figure 2 schematically pictures the pressure distribution in the present proposed hydrodynamic step bearing. The pressures are respectively linearly distributed in the "A" and "B" sub-zones and the maximum pressure occurs at the boundary of these two sub-zones.

4.2. Value Of ψ_{opt}

Figure 3 plots the ψ_{opt} versus r_h curve obtained in the present study. It is found that the value of ψ_{opt} only depends on r_h (but not dependent on K_u). The figure shows that the value of ψ_{opt} is linearly reduced with the increase of r_h.

4.3. The Load-Carrying Capacity at Optimum Condition

This section presents the calculated carried loads W_{slip} by the present bearing at optimum condition i.e. when $\psi=\psi_{opt}$ for the applicable r_h values and for several typical cases. They are compared with the carried loads W_{conv} of the conventional no-slippage hydrodynamic step bearing in the same operating conditions. When $\psi=\psi_{opt}$, Eqs. (32), (33) and (34) respectively become the following equations:

$$K_u>\frac{3}{2r_h^2} \tag{43}$$

$$K_u<\frac{3}{2r_h^2}+(1-\lambda_\tau)\left(1+r_h^{-\frac{3}{2}}\right) \tag{44}$$

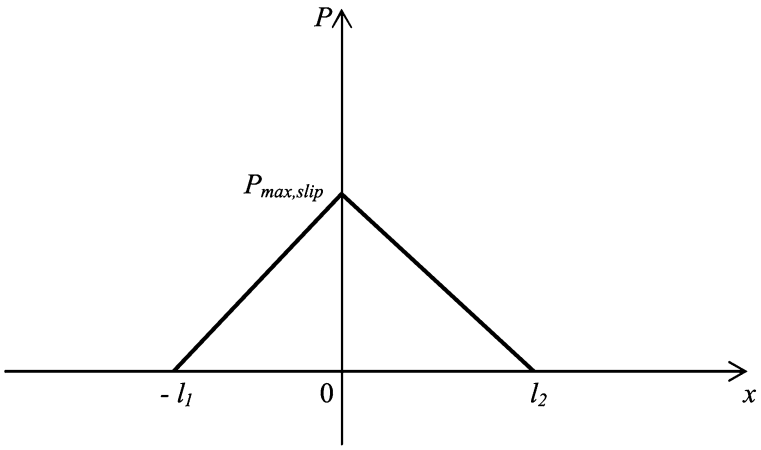

Fig. 2. Schematic picture of the fluid film pressure distribution in the present bearing.

$$\phi_\tau > 1 + \frac{G_1}{r_h}\left(1 + \frac{1}{\psi_{opt}}\right) \tag{45}$$

Four cases are calculated. The parameter values of these cases are respectively:

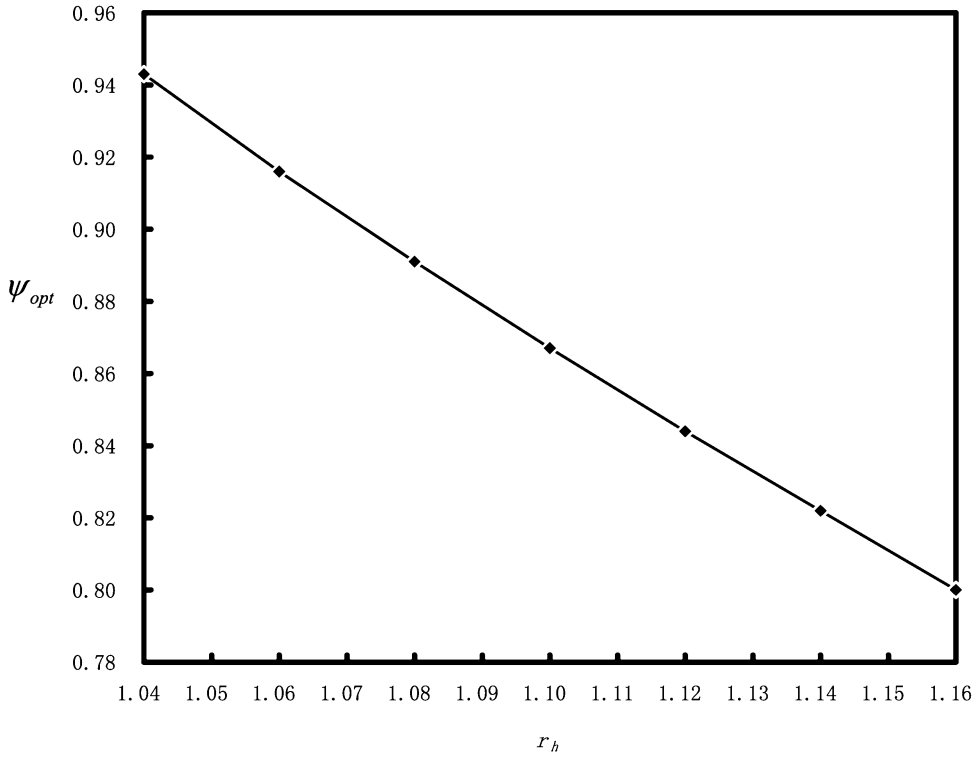

Fig. 3. The ψ_{opt} versus r_h curve.

Case 1 : $K_u = 2.0,\ \lambda_\tau = 0.5 (U = 0.9167),\ \phi_\tau = 2.0$

Case 2 : $K_u = 2.5,\ \lambda_\tau = 0.2 (U = 0.9333),\ \phi_\tau = 2.0$

Case 3 : $K_u = 1.6,\ \lambda_\tau = 0.1 (U = 0.5833),\ \phi_\tau = 2.0$

Case 4 : $K_u = 2.8,\ \lambda_\tau = 0.05 (U = 0.9583),\ \phi_\tau = 2.0$

Figure 4 plots the values of W_{slip} against r_h calculated for these four cases and compares them to the values of W_{conv} in the same operating conditions. It is shown that for these four cases boundary slippage significantly increases the load-carrying capacity of the hydrodynamic step bearing. For Cases 2 and 4, the increases are most significant and can reach 200~400%. This increasing effect tends to be reduced with the increase of r_h. For a given case, the value of W_{slip} is shown to be linearly increased with the increase of r_h.

4.4. Friction Coefficient

Figures 5(a) and (b) respectively plot the friction coefficients at the upper and lower bearing surfaces against r_h obtained for the present proposed bearing for the above mentioned four cases when $\psi = \psi_{opt}$ and $\alpha = 7.0E-4$. These friction coefficients are compared with the friction coefficients of the conventional no-slippage hydrodynamic step bearing in the same operating

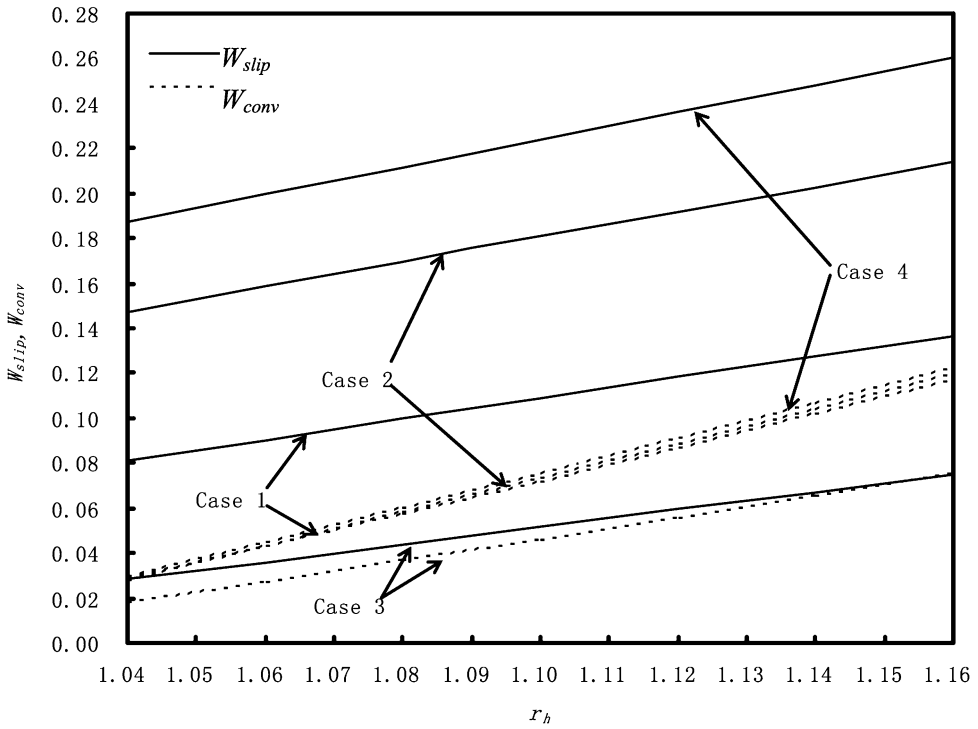

Fig. 4. Plot of the values of W_{slip} against r_h calculated for four typical cases and comparison of them with the values of W_{conv} in the same operating conditions when $\psi = \psi_{opt}$.

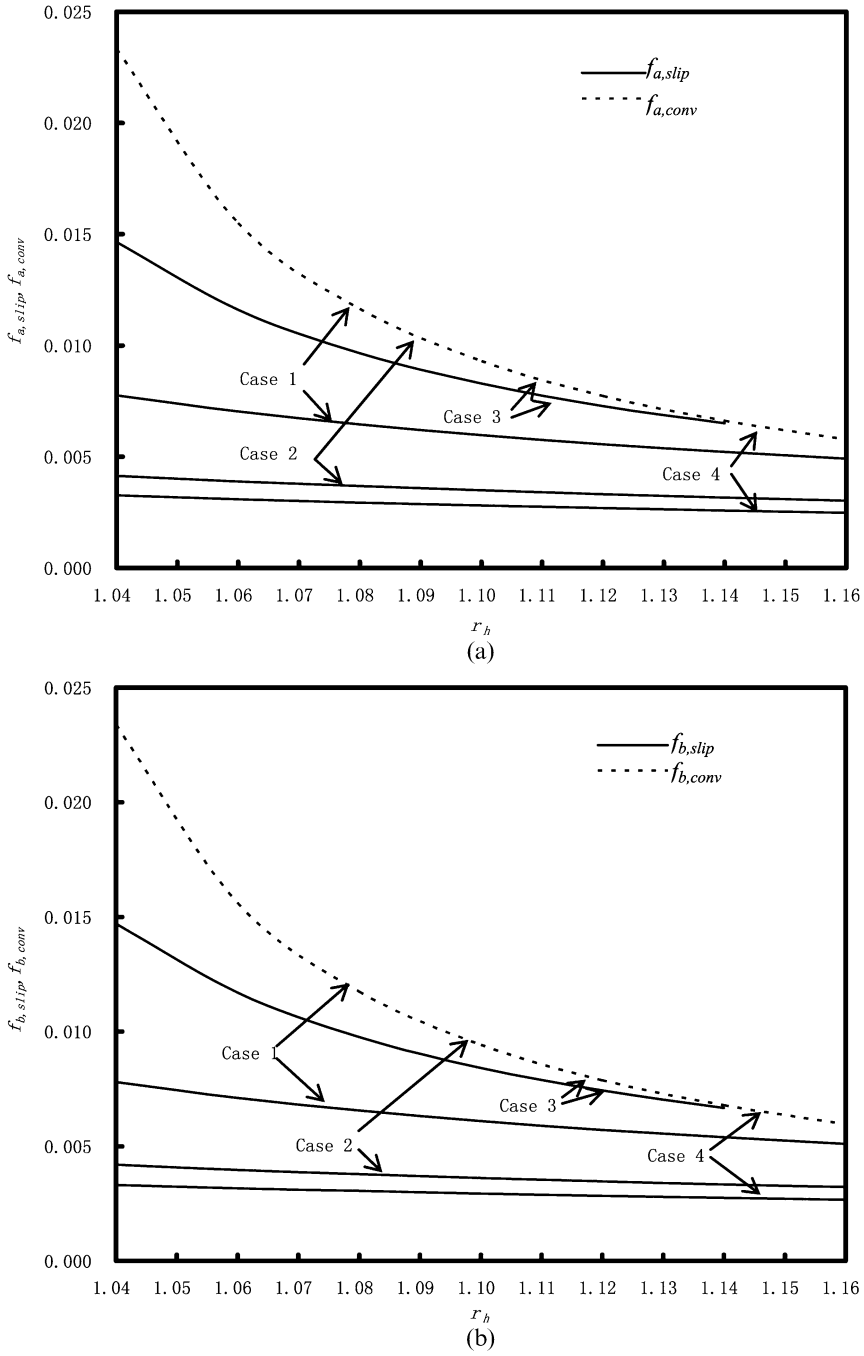

Fig. 5. Plot of the friction coefficients at the upper and lower bearing surfaces against r_h obtained for the present proposed bearing for four typical cases when $\psi = \psi_{opt}$ and $\alpha = 7.0E-4$ and comparison of them with the friction coefficients of the conventional no-slippage hydrodynamic step bearing in the same operating conditions.

conditions. It is shown that for these four cases boundary slippage significantly reduces the friction coefficients at both bearing surfaces in the present bearing. For Cases 2 and 4, the reductions are most significant and can reach 50~85%. This reduction effect tends to be reduced with the increase of r_h. For a given case, the friction coefficient in the present bearing is

shown to be reduced with the increase of r_h. Figures 4 and 5 give the implication that boundary slippage not only significantly increases the load-carrying capacity of the present bearing, at the same time it also significantly reduces the friction coefficient of the present bearing. These two effects seem to be strengthened or weakened synchronously.

5. CONCLUSIONS

The present paper proposes a new type of hydrodynamic step bearing by using boundary slippage. In this bearing, boundary slippage occurs at the stationary bearing surface in the fluid inlet zone due to the low interfacial shear strength at that bearing surface, it also occurs at the moving bearing surface in the fluid outlet zone due to the low interfacial shear strength at that bearing surface. At the other bearing surfaces, boundary slippage is absent due to the relatively high interfacial shear strengths at those surfaces. An analysis is derived for the load-carrying capacity and friction coefficient of this bearing. It is found that the load-carrying capacity of this bearing reaches the maximum when the value of the parameter ψ (which is the width ratio of the fluid outlet zone to the fluid inlet zone of the bearing) is optimum; The optimum ψ value for the load-carrying capacity is linearly reduced with the increase of r_h (which is the ratio of the fluid film thickness in the fluid inlet zone to that in the fluid outlet zone of the bearing).

The maximum load-carrying capacity of the bearing is derived and specially discussed. The carried loads and friction coefficients of this bearing at optimum ψ value are calculated for four typical cases. They are compared to those of the conventional no-slippage hydrodynamic step bearing in the same operating conditions. It is found that the introduction of boundary slippage is beneficial in the present bearing and it can significantly increase the load-carrying capacity but reduce the friction coefficient; The increase of the load-carrying capacity by boundary slippage can reach 200~400%, while the reduction of the friction coefficient by boundary slippage can be 50~85%. The effects of the increase of the load-carrying capacity and the reduction of the friction coefficient by boundary slippage seem to be strengthened or weakened synchronously. The study shows potential application values of boundary slippage in hydrodynamic step bearings.

ACKNOWLEDGMENTS

The author would like to express thanks to the Natural Science Foundation of Jiangsu Province, China (BK2008189) and the faculty project of Changzhou University (ZMF10020079).

REFERENCES

1. Zhang, Y.B. and Wen, S.Z., "An analysis of elastohydrodynamic lubrication with limiting shear stress: part I- theory and solutions," *Tribology Transactions*, Vol. 45, pp. 135–144, 2002.
2. Zhang, Y.B. and Wen, S. Z., "A lubrication deviation from the classical EHL theory by the lubricant viscoplasticity: part I- film thickness dependence," *Tribology Transactions*, Vol. 44, pp. 224–232, 2001.
3. Zhang, Y.B., "Mixed rheologies in elastohydrodynamic lubrication," *Industrial Lubrication and Tribology*, Vol. 56, pp. 88–106, 2004.
4. Zhang, Y.B. and Wen, S.Z., "An analysis of elastohydrodynamic lubrication with limiting shear stress: part II- load influence," *Tribology Transactions*, Vol. 45, pp. 211–216, 2002.

5. Guo, F. and Wong, P.L., ''An anomalous elastohydrodynamic lubrication film: inlet dimple,'' ASME *Journal of Tribology*, Vol. 127, pp. 425–434, 2005.
6. Fu, Z., Guo, F. and Wong, P. L., ''Non-classical elastohydrodynamic lubricating film shape under large slide-roll ratios,'' *Tribology Letters*, Vol. 27, pp. 211–219, 2007.
7. Yagi, K., Kyogoku, K. and Nakahara, T., ''Relationship between temperature distribution in EHL film and dimple formation,'' ASME *Journal of Tribology*, Vol. 127, pp. 658–665, 2005.
8. Rozeanu, L. and Snarsky, L., ''Effect of solid surface lubricant interaction on the load-carrying capacity of sliding bearings,'' ASME *Journal of Lubrication Technology*, Vol. 100, pp. 167–175, 1978.
9. Zhang, Y.B., ''Contact-fluid interfacial slippage in hydrodynamic lubricated contacts,'' *Journal of Molecular Liquids*, Vol. 128, pp. 99–104, 2006.
10. Zhang, Y.B., ''Boundary slippage for generating hydrodynamic load-carrying capacity,'' *Applied Mathematics and Mechanics*, Vol. 29, pp. 1155–1164, 2008.
11. Pinkus, O. and Sternlicht, B., *Theory of hydrodynamic lubrication*, McGraw-Hill, New York, 1961.